Analysis and implementation of fractional-order chaotic system with standard components

Juan Yao [a,b], Kunpeng Wang [a,*], Pengfei Huang [c], Liping Chen [d], J.A. Tenreiro Machado [e]

[a] School of Information and Engineering, Southwest University of Science and Technology, Mianyang 621010, China
[b] Department of Automation, University of Science and Technology of China, Hefei 230027, Anhui, China
[c] College of Automation, Chongqing University, Chongqing 400044, China
[d] School of Electrical Engineering and Automation, Hefei University of Technology, Hefei 230009, China
[e] Institute of Engineering, Polytechnic of Porto, Department of Electrical Engineering, R. Dr. António Bernardino de Almeida, 431, 4249-015 Porto, Portugal

GRAPHICAL ABSTRACT
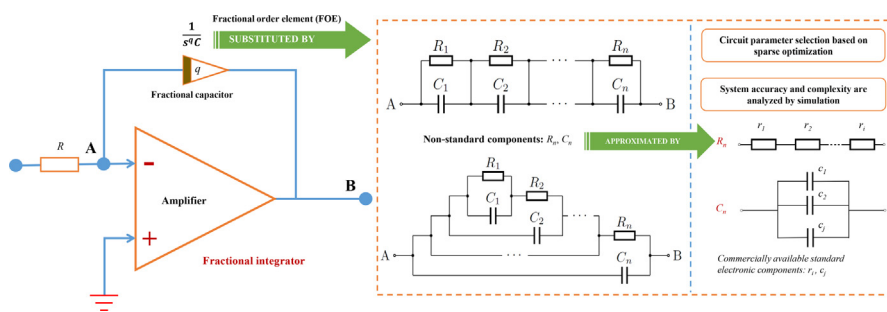
ARTICLE INFO

ABSTRACT

This paper is devoted to the problem of uncertainty in fractional-order Chaotic systems implemented by means of standard electronic components. The fractional order element (FOE) is typically substituted by one complex impedance network containing a huge number of discrete resistors and capacitors. In order to balance the complexity and accuracy of the circuit, a sparse optimization based parameter selection method is proposed. The random error and the uncertainty of system implementation are analyzed through numerical simulations. The effectiveness of the method is verified by numerical and circuit simulations, tested experimentally with electronic circuit implementations. The simulations and experiments show that the proposed method reduces the order of circuit systems and finds a minimum number for the combination of commercially available standard components.

Introduction

Fractional order calculus (FOC) is a generalization of the classical integer-order calculus arbitrary order [1]. The FOC offers a new view of modeling and understanding of the physical processes

since the fractional models can provide more adjustable parameters. The fractional-order PID controller, often denoted as $PI^\lambda D^\mu$ [2] and CRONE (Commande Robuste d'Ordre Non Entier) [3,4] algorithms, demonstrated to lead to control strategies more flexible than standard ones. In the area of electronics the fractional models describe dynamic characteristics of the semiconductors that are overlooked by integer models [5]. In recent decades, due to its powerful modeling capabilities, a variety of fractional models have been proposed and are widely used in electrical engineering [6], signal processing [7], neural network [8] and other fields.

Chaotic systems are a special type of nonlinear systems, that are highly unpredictable. Fractional-order chaotic systems exhibit even more complex behavior and play an important role in the encryption and decryption of secure communications [9,10]. Since Leon Chua introduced the celebrated Chua's circuit for the first time [11], the implementation of chaotic systems became a key topic. Following these ideas, V. Pham et al. [12] implemented a three-dimensional fractional-order chaotic system without equilibrium, P. Zhou et al. [13] designed an electronic circuit to obtain a 4-D fractional-order chaotic system. A. Akgul created a fractional order memcapacitor based chaotic oscillator with off the shelf components [14]. The system was capable of implementing Random Number Generators (RNG) using digital circuits based on integer and fractional-order chaotic systems [15]. The approximation problem of fractional-order systems with rational functions of low order have been raised and tried to be solved using optimization methods [16–18]. However, the complexity coupled with the uncertainty of chaos makes the realization of fractional-order chaotic systems hard to implement in engineering scenarios. In particular, complexity comes also from the fractional-order circuit units that are formed by a large number of electronic components. Indeed, the uncertainty is a consequence of two main aspects: (1) the highly unpredictability and non-linearity of the chaotic system, and (2) the errors between the nominal and the real values exhibited in electronic components in circuits.

The extra degree of freedom in fractional-order chaotic systems increases the difficulty when handling chaotic electronic circuits. The approaches for fractional-order circuit implementation can be roughly classified into three categories:

(1) **Traditional circuits with fractional components** Compared with the traditional integer-order calculus circuits, the fractional order elements (FOE) [19] are implemented by fractance capacitors [20,21], switched capacitors [22] or fractional coils [23].
(2) **Fractional behavior circuits with fractances or filter sections** The fractional-order circuit transfer functions can be realized by cascading a series of self-similar two-port networks [24–26], such as RC Ladder [27], Chain [28–30], and Tree [31] networks. Alternatively, the fractional-order Laplace operator s^α can be implemented using a weighted sum of first-order high-pass filter sections [32].
(3) **Digital circuits with discrete-time transformation** The fractional-order system is discretized by means of the Z-transform [33], following various schemes of discretization such as the trapezoidal (Tustin), Euler [34] and Al-Alaoui [35] rules, and have been widely used to implement chaotic systems using the Field Programmable Gate Array (FPGA) [36,37].

The first approach is a priori the most reasonable implementation method, but the fractional-order capacitors, inductors or coils are not easily obtained. Due to the inherent discretization error and narrow bandwidth of the implementation by the discrete-time system, in this paper we focus on the analog circuit implementation with fractances given their relatively wide bandwidth and high accuracy.

For approximating the fractional-order system with rational transfer function using fractances, a variety algorithms have been proposed [38,39] that can be classified into two categories:

(1) **Expansion** A fractional-order irrational function is expanded into a rational function with multiple poles and zeros by using the continued fraction expansions (CFE) [29], namely the Carlson's [26] and Matsuda's [40] methods.
(2) **Identification** The approximated rational function is obtained by fitting the frequency response of the theoretical irrational transfer function, such as the Oustaloup's [41] and Charef's [42] methods.

These methods lead to a transfer function approximation of the fractance that is implemented by a number of components. However, the uncertainty and circuit complexity that occur with the implementation procedure using real electronic components are not considered. Furthermore, the random errors caused by this uncertainty is detrimental for the performance of fractional-order chaotic systems with complex dynamics. The main motivation of this paper is to (i) analyze and model the influence of uncertainty on the circuits, and to (ii) develop a parameter optimization method to reduce the number of standard components and the overall uncertainty.

The remainder of this paper is organized as follows. In Section 2, the fraction calculus approximation methods and three typical structure of fractances are presented. In Section 3, the circuit implementation problem is formulated as an parameter optimization problem with sparsity and uncertainty constraints. Moreover, a fast numerical algorithm is proposed for this special nonlinear integer optimization problem. In Section 4, the influence in the chaotic system caused by the randomness of electronic component values is analyzed and modeled. In Section 5, the effectiveness of

Table 1
The zeros, poles and gain of $\widehat{H}^*(s)$ with $\delta = 2\text{dB}$.

q	N	Z	P	K
0.1	2	16.681, 2782.5594	10, 1668.1005, 278255.9402	100000
0.2	4	5.6234, 100, 1778.2794, 31622.7766	3.1623, 56.2341, 1000, 17782.7941, 316227.766	31622.7766
0.3	5	4.1596, 37.2759, 334.0485, 2993.5773, 26826.958	2.1544, 19.307, 173.0196, 1550.5158, 13894.9549, 124519.7085	4641.5888
0.4	6	3.8312, 26.1016, 177.8279, 1211.5277, 8254.0419, 56234.1325	1.7783, 12.1153, 82.5404, 562.3413, 3831.1868, 26101.5722, 177827.941	1778.2794
0.5	6	3.9811, 25.1189, 158.4893, 1000, 6309.5734, 39810.7171	1.5849, 10, 63.0957, 398.1072, 2511.8864, 15848.9319, 100000	398.1072
0.6	6	4.6416, 31.6228, 215.4435, 1467.7993, 10000, 68129.2069	1.4678, 10, 68.1292, 464.1589, 3162.2777, 21544.3469, 146779.9268	146.7799
0.7	6	6.4495, 57.7969, 517.9475, 4641.5888, 41595.6216, 372759.372	1.3895, 12.452, 111.5884, 1000, 8961.505, 80308.5722, 719685.673	71.9686
0.8	4	13.3352, 237.1374, 4216.965, 74989.4209	1.3335, 23.7137, 421.6965, 7498.9421, 133352.1432	13.3352
0.9	3	129.155, 21544.3469, 3593813.6638	1.2915, 215.4435, 35938.1366, 5994842.5032	5.9948

the proposed method is analyzed and verified by simulations and experiments hardware. In Section 6, the paper is concluded.

Preliminaries

In the Laplace domain, the transfer function of the linear fractional integrator of order $0 < q < 1$ can be written as $H(s) = 1/s^q$, and $s = j\omega$ refers to the complex frequency. From the point of view of engineering the implementation can be represented as [42]:

$$H(s) = \frac{1}{(1 + \tau_0 s)^q}, \tag{1}$$

where the positive real number τ_0 is a relaxation time constant, and q is the fractional-order.

Fractional order integrator approximation

In the Laplace domain, the fractional slope of -20α dB/decade of $H(s)$ in a log–log plot can be approximated by a series of asymptotic lines with alternate slopes of -20 dB/decade and 0 dB/decade [42]. For the convenience of description, we call it as "pole/zero" method. Then, the transfer function can rewritten as:

$$H(s) = \lim_{N \to \infty} \frac{\prod_{i=0}^{N-1}\left(1 + \frac{s}{z_i}\right)}{\prod_{i=0}^{N-1}\left(1 + \frac{s}{p_i}\right)} \approx \frac{\prod_{i=0}^{N-1}\left(1 + \frac{s}{z_i}\right)}{\prod_{i=0}^{N}\left(1 + \frac{s}{p_i}\right)} \tag{2}$$

where $(N + 1)$ denotes the total number of singularities (poles) that are associated with the maximum frequency ω_{max}, so that:

$$N = \left\lfloor \frac{\log\left(\frac{\omega_{max}}{p_0}\right)}{\log(ab)} \right\rfloor + 1, \tag{3}$$

where $\lfloor \cdot \rfloor$ denotes the floor function, $p_0 = p_T 10^{(\delta/20q)}$ is the first polar of the transfer function, and $\omega_c = p_T = \frac{1}{\tau_0}$ is the corner frequency also be called as $-3q$ dB/decade point. Besides, $z_i = p_{i-1}a$ and $p_i = z_{i-1}b$ denote the i'th zero and pole of the transfer function, respectively, and $a = 10^{[\delta/10(1-q)]}, b = 10^{\delta/10q}$. The value of δ (in dB) is a positive number that stands for the maximum discrepancy between the desired transfer function $H(s)$ and the approximated transfer function $\widehat{H}(s)$ given by:

$$\widehat{H}(s) = \frac{\prod_{i=0}^{N-1}\left(1 + \frac{s}{(ab)^i ap_0}\right)}{\prod_{i=0}^{N}\left(1 + \frac{s}{(ab)^i p_0}\right)}. \tag{4}$$

Clearly, the smaller δ, the more accurate the approximation, but the complexity of the transfer function rises significantly. In addition, the frequency range of $\widehat{H}(s)$ is $\omega \in [\omega_c, \omega_{max}), \omega_{max} = p_T 10^{N\left(\frac{\delta}{10q} + \frac{\delta}{10(1-q)}\right) + \frac{\delta}{20q}}$. To maintain the balance between complexity and accuracy, the discrepancy can be set to value such as $\delta = 2$ dB. Based on this assumption, we set $\omega_c = p_T = 1/\tau_0 = 10^0$ rad/s, $\omega_{max} = 10^5$ rad/s, the zeros (Z), poles (P) and gains (K) of $\widehat{H}(s)$ are given in Table 1.

The structure of fractances

Integer calculus can be realized with electric circuits, using standard components such as contain Operational Amplifiers (OPA), resistors and capacitors. However, for fractional calculus, the realization depends on a specific RC circuit network with fractal characteristics.

Fractal circuits have self-similarity and are formed by several topologically similar layers with resistors and capacitors. The number of layers is related to the number of poles and zeros of the approximated transfer function. The most common used approximations of fractances consist of the chain, RC domino ladder and RC binary tree structures [43].

The chain structure

As shown in Fig. 1, the basic unit is the parallel association of resistor and capacitor circuits, that can be regarded as layers of the fractance. According to the two-port network theory, the transfer function of this fractance in the Laplace domain is:

$$H^{RC}(s) = \frac{1}{C_1 s + \frac{1}{R_1}} + \frac{1}{C_2 s + \frac{1}{R_2}} + \cdots + \frac{1}{C_n s + \frac{1}{R_n}}. \tag{5}$$

The tree structure

As shown in Fig. 2, the fractance is organized according to binary tree structure. Each layer's resistor and capacitor connects to another parallel circuit unit to form a new layer. In the Laplace domain the transfer function of this fractance is:

$$H^{RC}(s) = \frac{1}{\frac{1}{R_1 + \frac{1}{\frac{1}{R_2 + \cdots} + \frac{1}{\frac{1}{C_2 s} + \cdots}}} + \frac{1}{\frac{1}{C_1 s} + \frac{1}{\frac{1}{R3 + \cdots} + \frac{1}{\frac{1}{C_3 s} + \cdots}}}}. \tag{6}$$
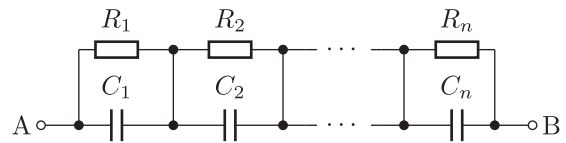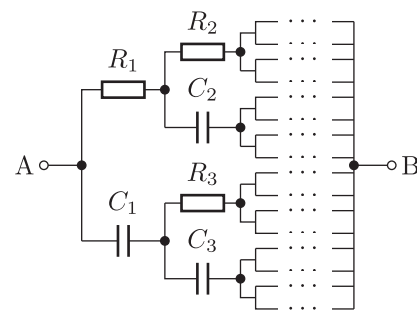

Fig. 1. The RC chain structure.
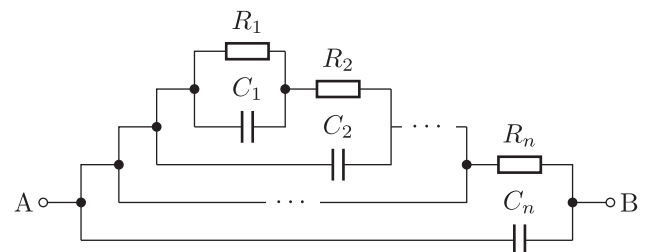

Fig. 2. The RC binary tree structure.

Fig. 3. The RC domino ladder structure.

The ladder structure

As shown in Fig. 3, each layer is in series with one resistor and then includes a parallel connection to one capacitor to form another layer. In the Laplace domain the transfer function of this tree network is:

$$H^{RC}(s) = \cfrac{1}{\cfrac{1}{\cfrac{1}{\frac{1}{\frac{1}{R_1} + sC_1} + R_2} + sC_2} + R_3} + sC_3 + \cdots. \tag{7}$$

Parameter selection with sparse optimization

As mentioned in Section 2, the fractional-order calculus can be approximated by integer transfer function with multiple poles and zeros and the approximated transfer function can be realized with fractance circuits. Due to the sensitiveness to initial conditions and system parameters exhibited by chaotic system, the circuit implementation requires an high accuracy. However, especially in analogue circuits, the tolerances of the electronic components and the background noise bring the system to errors and uncertainties. Furthermore, the error introduced by the process of approximation can not be neglected and, consequently, the circuit implementation of chaotic systems poses severe problems.

The circuit implementation of fractional-order calculus rely on fractance circuits consisting of $K_r \in \mathbb{N}$ resistors and $K_c \in \mathbb{N}$ capacities. Let the transfer function $H^{RC}(s)$ equal the approximated transfer function $\widehat{H}(s)$, so that:

$$C_r \cdot H^{RC}(s) = \widehat{H}(s), \tag{8}$$

where $C_r \in \mathbb{R}_>$ is a gain adjustment factor, $\mathbb{R}_> = \{x \in \mathbb{R} | x > 0\}$ represents the set of positive real numbers. The analytically solution of $\mathbf{r} = (R_1, R_2, \ldots, R_{K_r})^T$ and $\mathbf{c} = (C_1, C_2, \ldots, C_{K_c})^T$ is not always achievable by solving a homogeneous equation that is build by equating the corresponding coefficients when the system order is larger than 3. Moreover, components with the calculated values may not be commercially available. By other words, the calculated value of resistors and capacitors may not be the standard values of electronic components. For overcoming this problem, there are two solutions:

- Ordering special manufacturing for values of non-standard capacitors and resistors.
- Combining the standard electronic components to approximate the non-standard theoretical value.

The first solution leads to a simpler circuit design and higher precision, but with high cost and long manufacturing cycle problems. The second solution is a more economic and time-saving way of implementation, but the number of electronic components used in the circuit may eventually be very large. According to the discussion above, the amount of standard electronic components used for substitution needs to be controlled to further limit the accumulative error and to increase the stability of the whole circuit system.

For this purpose, a sparse optimization method is developed in the follow-up. Commercially unavailable resistors or capacitors can always be approximated by the combination of available E-series electronic resistors $\boldsymbol{\alpha} = (\alpha_1, \alpha_2, \ldots, \alpha_{M_r})^T$ and capacitors $\boldsymbol{\beta} = (\beta_1, \beta_2, \ldots, \beta_{M_c})^T$:

$$\underbrace{\begin{bmatrix} \mathbf{r} \\ \mathbf{c} \end{bmatrix}}_{\mathbf{y}} = \underbrace{\begin{bmatrix} \mathbf{A} & \\ & \mathbf{B} \end{bmatrix}}_{\mathbf{X}} \cdot \underbrace{\begin{bmatrix} \boldsymbol{\alpha} \\ \boldsymbol{\beta} \end{bmatrix}}_{\boldsymbol{\psi}} + \underbrace{\begin{bmatrix} \mathbf{u} \\ \mathbf{v} \end{bmatrix}}_{\boldsymbol{\eta}} \boldsymbol{\eta}, \tag{9}$$

where α_i and β_i denote the values of standard resistors and capacitors respectively. The symbols M_r and M_c stand for the number of the E-series commercially available standard resistors and capacitors, respectively. Moreover, $\mathbf{A} \in \mathbb{Z}_{\geqslant}^{K_r \times M_r}$ and $\mathbf{B} \in \mathbb{Z}_{\geqslant}^{K_c \times M_c}$ are coefficient matrices, $\mathbb{Z}_{\geqslant} = \{x \in \mathbb{Z} | x \geqslant 0\}$ represents the set of non-negative integers, $\mathbf{u} \in \mathbb{R}_{\geqslant}^{K_r}$ and $\mathbf{v} \in \mathbb{R}_{\geqslant}^{K_c}$ are the corresponding residual vectors, $\mathbb{R}_{\geqslant} = \{x \in \mathbb{R} | x \geqslant 0\}$ represents the set of non-negative real numbers, $\mathbf{y} \in \mathbb{R}_>^K$ is the theoretical component values, $\mathbf{X} \in \mathbb{Z}_{\geqslant}^{K \times M}$, so that $K = K_r + K_c$ and $M = M_c + M_r$.

The potential value of the m'th electronic component ψ_m is a random variable $\psi_m \sim \mathcal{N}(\mu_m, \sigma_m^2)$ that follows the normal distribution. However, the actual situation is that a value falling outside the limits are scrapped or reworked in the manufacturing process and so the inspected electronic component follows a truncated normal distribution. Its value lies within the interval $\psi_m \in [a, b]$ [44], with $a = \mu_m - 3\sigma_m, b = \mu_m + 3\sigma_m, m = 1, 2, \ldots, M$, where μ_m and ε_m are the nominal value and the tolerance of the component, respectively. According to the definition of international standard IEC-60063 [45], we have $3\sigma_m = \varepsilon_m \cdot \psi_m$. The probability density function (PDF) of ψ_m can be given by:

$$f(\psi_m; \mu_m, \sigma_m, a, b) = \begin{cases} \dfrac{\phi\left(\frac{\psi_m - \mu_m}{\sigma_m}\right)}{\sigma_m \cdot \left(\Phi\left(\frac{b - \mu_m}{\sigma_m}\right) - \Phi\left(\frac{a - \mu_m}{\sigma_m}\right)\right)}, & a \leqslant \psi_m \leqslant b \\ 0, & \text{otherwise} \end{cases}. \tag{10}$$

Let us consider $\phi(\xi) = \frac{1}{\sqrt{2\pi}} \exp(-\xi^2/2)$ and $\Phi(\xi) = \frac{1}{2}\left(1 + erf\left(\xi/\sqrt{2}\right)\right)$ for the PDF and cumulative distribution function of the standard normal distribution, respectively, with $erf(\xi) = \frac{2}{\sqrt{\pi}} \int_0^\xi e^{-t^2} dt$ standing for the Gauss error function.

Then the mean and variance of truncated random variable ψ_m can be written as [46]:

$$\hat{\mu}_m = \mu_m + \sigma_m \frac{\phi(\alpha) - \phi(\beta)}{\Phi(\beta) - \Phi(\alpha)}, \hat{\sigma}_m^2$$
$$= \sigma_m^2 \left[1 + \frac{\alpha\phi(\alpha) - \beta\phi(\beta)}{\Phi(\beta) - \Phi(\alpha)} - \left(\frac{\phi(\alpha) - \phi(\beta)}{\Phi(\beta) - \Phi(\alpha)}\right)^2\right], \tag{11}$$

where $\alpha = (a - \mu_m)/\sigma_m$ and $\beta = (b - \mu_m)/\sigma_m$.

Since $erf(\xi)$ is an odd function and $\alpha = -\beta = -3$, we have $erf(-\xi) = -erf(\xi), \phi(\alpha) = \phi(\beta) = \exp(-9/2)/\sqrt{2\pi}$ and $\Phi(\beta) - \Phi(\alpha) = erf\left(3/\sqrt{2}\right)$. Finally, the mean and variance of ψ_m can be simplified as:

$$\hat{\mu}_m = \mu_m, \hat{\sigma}_m^2 = \sigma_m^2\left(1 - 6 \cdot \frac{\exp(-9/2)}{\sqrt{2\pi} \cdot erf\left(3/\sqrt{2}\right)}\right) \approx 0.97 \cdot \sigma_m^2. \tag{12}$$

Then the k'th element η_k of residual vector $\boldsymbol{\eta} \in \mathbb{R}^K, k = 1, 2, \ldots, K$, is a random variable with the mean and variance given by:

$$\mu_{\eta_k} = y_k - x_{k,*} \cdot \boldsymbol{\psi}, \sigma_{\eta_k}^2 \propto x_{k,*} \cdot \boldsymbol{\sigma}_\psi^2, \tag{13}$$

where y_k is the theoretical value of k'th component, $\boldsymbol{\sigma}_\psi = (\hat{\sigma}_1, \hat{\sigma}_2, \ldots, \hat{\sigma}_M)^T$ is the standard deviation vector of all the standard electronic components, and $x_{k,*}$ refers to the k'th row of $\mathbf{X}$. Here we take the ratio of the sum of the standard deviation $\mathbf{x}_{k,*}\boldsymbol{\sigma}_\psi$ and the k'th component value $y_k = \mathbf{x}_{k,*}\boldsymbol{\psi}$:

$$c_k = \frac{\mathbf{x}_{k,*}\boldsymbol{\sigma}_\psi}{\mathbf{x}_{k,*}\boldsymbol{\psi}}, \tag{14}$$

as the indication of uncertainty in the circuit implementation procedure. Generally speaking, the larger the value of c_k, the higher the variability of y_k, and the greater the probability of failure. To simplify, the sum of ratio c_k can be obtained by:

$$\|\mathbf{c}\|_1 = \left(\mathbf{X}\boldsymbol{\sigma}_\psi\right)^T \cdot \left(\mathbf{X}\boldsymbol{\psi}\right)^{-1}, \tag{15}$$

where $\mathbf{c} = (c_1, c_2, \ldots, c_K)^T$ denotes the ratio vector, and $\|\cdot\|_1$ refers to the "entry-wise" ℓ_1-norm.

Definition 1. The complexity of the circuit is defined by the average number of standard electronic components used in each circuit parameter implementation, that is:

$$\text{CM} := \lambda \frac{1}{M_r} \|\mathbf{A}\|_1 + (1 - \lambda) \frac{1}{M_c} \|\mathbf{B}\|_1 = \|\mathbf{XW}\|_1, \tag{16}$$

where $\mathbf{W}$ is the corresponding weight matrix, and $\|\mathbf{A}\|_1$ and $\|\mathbf{B}\|_1$ denote the total number of resistors and capacitors usage in implementation of the analytical solution of circuit parameters $\mathbf{r}$ and $\mathbf{c}$, respectively. The parameter $0 < \lambda < 1$ is a trade-off between the different types of parameters.

Given a suitable initial values $\mathbf{y}_0$ of the components used, the gain factor $C_r = C_{r0}$, and the frequency band $\omega \in [\omega_c, \omega_{max})$, the circuit parameter matrix $\mathbf{X}$ can be derived by a sparse optimization problem defined as:

$$\min_{C_r, \mathbf{y}} (\mathbf{X}\boldsymbol{\sigma}_\psi)^T \cdot (\mathbf{X}\boldsymbol{\psi})^{-1} + \lambda_1 \cdot \|\mathbf{XW}\|_1, \tag{17a}$$

$$\text{s.t.} \, C_r \in \mathbb{R}_>, \mathbf{y} \in \mathbb{R}_>^K, \tag{17b}$$

$$\sup\{D(\omega) | \omega \in [\omega_c, \omega_{max}), \mathbf{X}\} \leqslant \delta$$

and the parameter matrix $\mathbf{X} \in \mathbb{Z}_\geqslant^{K \times M}$ can be deduced from $\mathbf{y}$ by:

$$x_{i,j} = \begin{cases} \lfloor e_{i,j}/\psi_j \rfloor, & \text{for } e_{i,j} \geqslant \zeta_{i,j} \\ 0, & \text{otherwise} \end{cases}, \tag{18}$$

where $e_{i,j} = y_i - \sum_{m=1}^{j-1} x_{i,m} \cdot \psi_m$ represents the j'th residual of y_i, $\zeta_{i,j} = \sum_{m=1}^{j-1} x_{i,m} \cdot \sigma_m$ is defined as the uncertainty within one standard deviation of y_i, $i = 1, 2, \ldots, K, j = 1, 2, \ldots, M$, and $\lfloor \cdot \rfloor$ denotes the floor function. The first term of Eq. (17a) gives the uncertainty in the circuit implementation of the transfer function $H(s)$, and the regularization term $\|\mathbf{XW}\|_1$ stands for the average number of standard electronics components used in the fractance implementation. The positive parameter λ_1 introduces a trade-off between implementation uncertainty and sparsity. Moreover, $D(\omega) = |\widehat{A}_{vdB}(\omega) - A_{vdB}(\omega)|$ measures the magnitude discrepancy between $H(s)$ and $\widehat{H}(s)$, where $A_{vdB}(\omega) = 20 \cdot \log|H(j\omega)|$ and $\widehat{A}_{vdB}(\omega) = 20 \cdot \log|C_r \cdot \widehat{H}(j\omega)|$ are the magnitude of the transfer functions $H(s)$ and $\widehat{H}(s)$, respectively, having in mind that the inequality constraint in Eq. (17b) limits the maximum discrepancy between them.

The objective function in Eq. (17a) is a linear function to be minimized. Nonetheless, the constraints involve integer variables, real-valued variables and nonlinear functions. Thus, the minimization problem of Eq. (17) is a mixed integer nonlinear program (MINLP). The problem refers to nonlinear programming with discrete and continuous variables, and has been used in various fields, such as in engineering, finance and manufacturing. It is challenging to solve theoretically this *NP*-hard combinational problem that in general is not feasible [47]. We can introduce a barrier function to remove the inequality constraint, and then the optimization problem of Eq. (17) can be re-formulated as:

$$\min_{C_r, \mathbf{y}} (\mathbf{X}\boldsymbol{\sigma}_\psi)^T \cdot (\mathbf{X}\boldsymbol{\psi})^{-1} + \lambda_1 \cdot \|\mathbf{XW}\|_1 + \mu \cdot g(\mathbf{X}), \text{s.t.} \, C_r \in \mathbb{R}_{>0}, \mathbf{y} \in \mathbb{R}^K \tag{19}$$

where the barrier function $g(\mathbf{X})$ is defined as:

$$g(\mathbf{X}) = \begin{cases} \log_p(D_\delta) + 1, & \text{for } D_\delta > 1 \\ D_\delta^2, & \text{otherwise} \end{cases}, \tag{20}$$

the ratio $D_\delta = \sup\{D(\omega)/\delta | \omega \in [\omega_c, \omega_{max}), \mathbf{X}\}$ denotes the relative maximum discrepancy, $p \in (1, +\infty)$, and $\mu \in \mathbb{R}_>$ is a free parameter. In the discrete domain, D_δ can be obtained by

$$D_\delta = \arg\max_{\omega, \mathbf{X}} \{D(\omega_i)/\delta\}, \tag{21}$$

where $\boldsymbol{\omega} = (\omega_1, \omega_2, \ldots, \omega_{N_\omega})^T \in \mathbb{R}_>^{N_\omega}$ consists of N_ω frequency points sampling from the frequency band $\omega_i \in [\omega_c, \omega_{max})$. This optimization problem is not equivalent to Eq. (17), but as $\mu \to 0$ it can be seen as an approximation. In this paper we set $p = 1.01$ and $\mu = 1$.

The initial values $\mathbf{y}_0$ and C_{r0} can be estimated by minimizing the following objective function which given by:

$$J(C_r, \mathbf{y}) = \sum_{i=1}^{N_\omega} \left\{ \left(|C_r \cdot \widehat{H}(j\omega_i)| - |H(j\omega_i)| \right)^2 \right.$$
$$\left. + \lambda_2 \cdot \left(\text{Im}\left(C_r \cdot \widehat{H}(j\omega_i) \right) - \text{Im}(H(j\omega_i))^2 \right) \right\}, \tag{22}$$

where $\lambda_2 \in \mathbb{R}_>$ is a parameter to trade-off between the error of magnitude and phase. Then, according to Eq. (18), for $\mathbf{y}_0 \approx \mathbf{X}_0 \cdot \boldsymbol{\psi}$, we deduce an approximate solution of the initial parameter matrix $\mathbf{X}_0$.

To minimize the objective function (17) with nonlinear and discrete constrains, a Genetic Algorithm (GA) [48,49] is used. GAs have achieved some success in the fractional calculus field to optimize fractional controllers [50], approximate fractional derivatives [51] and implement fractional-order inductive elements [52]. The circuit parameter matrix $\mathbf{X}$ and the gain adjustment factor C_r are encoded as genomes, with every genome being interpreted as a potential solution for the sparse optimization problem.

Uncertainty measurement in chaotic circuit system implementation

As mentioned previously, the uncertainty in the circuit implementation of $\widehat{H}(s)$ will significantly influence the quality of chaotic system and, in most cases, the circuit complexity is the main cause of uncertainty. In order to accurately evaluate the impact of the circuit complexity and component tolerance on the uncertainty, we now define performance criteria of chaotic circuit system implementation. The failure of the circuit implementation is mainly reflected in two aspects: (1) the approximation error of fractional order operators is larger than the set range, and (2) chaos degenerates or chaotic behavior disappears. The uncertainty will be defined in terms of these two aspects, respectively.

Approximation error of fractional order operators

Definition 2. The uncertainty is defined as the failure probability of the circuit implementation with a given parameter $\mathbf{X}$,

$$\text{UC}(\mathbf{X}) := p(D_\delta > 1|\mathbf{X}), \tag{23}$$

where D_δ denotes the maximum magnitude discrepancy relative to δ between $H(s)$ and $\widehat{H}(s)$.

In order to calculate the probability in Eq. (23), we need to first derive the amplitude probability distribution $p\left(|\widehat{H}(j\omega)|\right)$ of $\widehat{H}(s)$ defined in Eqs. (5)–(7) by a given circuit parameter matrix $\mathbf{X}$. Taking an implementation of a second order system of Eq. (5) for example:

$$\widehat{H}(s) = \frac{1}{C_1 s + \frac{1}{R_1}} + \frac{1}{C_2 s + \frac{1}{R_2}}$$
$$= \frac{R_1 R_2 (C_1 + C_2)s + R_1 + R_2}{R_1 R_2 C_1 C_2 s^2 + (R_1 C_1 + R_2 C_2)s + 1}, \tag{24}$$

as mentioned above, the random variables R and C are truncated normal distributions, and their probability density function are

given by Eq. (10). However, the distribution of product and ratio of more than two independent, continuous random truncated normal variables (e.g., $p(R_1R_2(C_1 + C_2))$ and $p(R_1R_2C_1C_2)$), becomes complicated with cascading operations [53,54] and, therefore, the probability of uncertainty cannot be directly calculated for a given circuit parameter matrix $\mathbf{X}$. However, it can be approximately calculated by sampling from a series truncated normal distribution. We give an estimation algorithm of the uncertainty probability using the Monte Carlo simulation method as shown in Table 2.

A truncated normal random variable ψ_m that follows the distribution truncated to the range $[a, b]$ is defined as:

$$\psi_m = \Phi^{-1}(\Phi(\alpha) + U \cdot (\Phi(\beta) - \Phi(\alpha))) \cdot \sigma_m + \mu_m$$
$$= \Phi^{-1}\left(1/2 + U \cdot erf\left(3/\sqrt{2}\right)\right) \cdot \sigma_m + \mu_m, \qquad (25)$$

where $\Phi^{-1}(\cdot)$ is the inverse of the cumulative distribution function $\Phi(\cdot)$, and U is a uniform random variable in range $[-1/2, 1/2]$. The classic inverse transform method for generating a random variable following the density function of Eq. (10) may fail in the sampling at the tail of distribution [55], or may be much too slow [56]. In order to accelerate the sampling of multiple truncated normal distribution variables, we use a table-based fast sampling algorithm that proposed by Chopin [57].

The relative maximum magnitude discrepancy D_δ can be calculated using the random variates $\boldsymbol{\psi} = (\psi_1, \ldots, \psi_M)^T$ and the circuit parameter matrix $\mathbf{X}$. The k'th component's value y_k of the transfer function $\widehat{H}(s)$ can be determined by $y_k = \mathbf{x}_{k,*}\boldsymbol{\psi}$, and the implementation uncertainty of system can be redefined as:

$$UC_i(\mathbf{X}) := \begin{cases} 1, & D_\delta > 1 \\ 0, & \text{otherwise} \end{cases}. \qquad (26)$$

Chaos degenerates or chaotic behavior disappears

From the perspective of whether chaotic behavior can be maintained in the process of chaotic system realization, according to [58], a necessary condition for the fractional system to remain chaotic can be adopted to indicate the uncertainty.

Definition 3. For a given fractional-order system $\frac{d^q x}{dt^q} = f(x)$, the uncertainty in the circuit implementation of this system with a given parameter $\mathbf{X}$ can be defined as follows

Table 2
Monte Carlo based uncertainty estimation algorithm.

Initialization:
1: **INIT** system order q, maximum discrepancy δ, number of the singularities N, parameter matrix $\mathbf{X}$, Gain factor C_r, tolerance of standard components ε, maximum iteration steps n.
2: **SET** iteration count i to zero.

Iteration:
3: **WHILE** $i < n$ **THEN**
4:    Generate all the random variate $\psi_m, 0 \leqslant m \leqslant M$ of standard electronic components ψ by Eq. (25).
5:    Calculate the value of components used in transfer function $\widehat{H}(s)$ by $\mathbf{y} = \mathbf{X}\boldsymbol{\psi}$.
6:    Update $D_\delta = \arg\max_{\omega, \mathbf{X}} \{D(\omega_i)/\delta\}$ or q_{sup} by using $\widehat{H}(s)$.
7:    **IF** $D_\delta > 1$ **OR** $q \leqslant q_{sup}$ **THEN**
         $UC_i(\mathbf{X}) = 1$.
       ELSE IF $D_\delta \leqslant 1$ **OR** $q > q_{sup}$ **THEN**
         $UC_i(\mathbf{X}) = 0$.
       END IF
8:    $i := i + 1$.
9: **ENDWHILE**
10: Compute the estimated value of implementation uncertainty:
     $\widehat{UC} = \frac{1}{n}\sum_{i=1}^{n} UC_i(\mathbf{X})$.

$$UC(\mathbf{X}) := p(q \leqslant q_{sup}|\mathbf{X}), \qquad (27)$$

where $q_{sup} = \frac{2}{\pi}\text{actan}\left(\frac{|\text{Im}(\lambda_u)|}{\text{Re}(\lambda_u)}\right)$, and λ_u is an unstable eigenvalue of one of the saddle points of index 2.

Similarly, the unstable eigenvalue λ_u can be evaluated by randomly sampling from parameter matrix $\mathbf{X}$, and then Eq. (27) can be rewritten as:

$$UC_i(\mathbf{X}) := \begin{cases} 1, & q \leqslant q_{sup} \\ 0, & \text{otherwise} \end{cases}. \qquad (28)$$

Finally, the estimated value of implementation uncertainty can be obtained by taking $UC_i(\mathbf{X})$ as a statistic after n times direct simulations:

$$\widehat{UC} = \frac{1}{n}\sum_{i=1}^{n} UC_i(\mathbf{X}). \qquad (29)$$

Experiments and analysis

To verify the effectiveness of the proposed method, a number of numerical and circuit simulations followed by experiments with electronic circuit implementations are conducted on arbitrary fractional order and three types of fractance structure. Both performance criteria of circuit complexity and uncertainty are compared with the "pole/zero" approximation method defined in Eq. (4). The source code is available at: https://github.com/msp-lab/sofocs.

Given the same fractional order q, the numerical simulations in this section can be divided into three categories: minimum system order N requirement, circuit complexity comparison, and circuit uncertainty comparison in the implementation procedure. In the circuit simulation and electronic circuit implementation experiments, a fractional-order chaotic circuit for multi-scroll attractor is obtained by means of the "pole/zero" approximation and the proposed sparse optimization methods.

Minimum system order requirement comparison

For a given pair of fractional order q and maximum discrepancy δ, we compare the approximation ability of the proposed and the "pole/zero" methods. A comparative experiment is conducted to test the minimum number of fractance orders required by the two methods for 1 dB, 2 dB and 3 dB maximum discrepancy error tolerance. In general, we set the frequency range as $\omega \in \left[10^{-2}, 10^2\right)$ and $\tau_0 = 100$.

As shown in Fig. 4, the proposed method requires fewer orders of fractances than the "pole/zero" method. In other words, the method can always find a potential low-order circuit system to achieve the same fractional order, and has the advantage of reducing circuit complexity. In addition, lower system order requirements mean a more parsimonious use of topologically similar layers in fractal circuit. Indeed, the proposed method can reduce to about half number of layers and that is more evident as the accuracy of implementation increases.

Circuit complexity comparison

The complexity of the circuit is related to the order of the fractance system N and the number of standard components used to implement each ideal component. Here, we evaluate the circuit complexity with the total amount and the average number of components usage for the same fractional order.

As shown in Fig. 5a, the proposed method has the smallest usage of ideal component implementation, and can save about 60% of components in most cases. This result means not only that
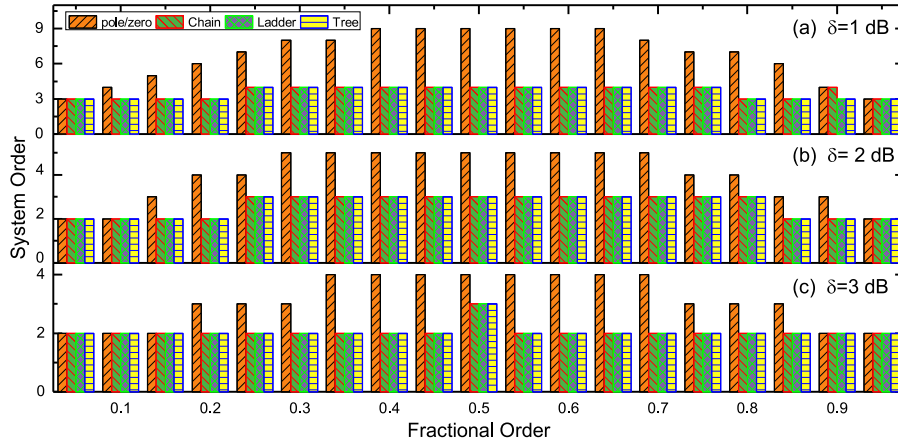
Fig. 4. The minimum system order requirement: comparison between the three types of fractance structure using the proposed and the "pole/zero" methods.

the circuit complexity is reduced and is easier to implement, but also that lower circuit noise is obtained and that the accuracy and reliability of the circuit are improved. Meanwhile, as shown in Fig. 5b, for an actual implementation of an ideal resistor or capacitor, the proposed method uses quantities inferior to those required by the "pole/zero" method, for most cases.

Circuit implementation uncertainty comparison

Since the value of the components actually used in the fractance circuit realization is a random variable obeying the truncated normal distribution, the change of the zero-pole position of the transfer function is unavoidable, and thus the quality of the circuit cannot be completely guaranteed. We use the uncertainty measurement method given in Section 4 (Definition 2) to investigate the uncertainty in the implementation procedure of the transform function derived by the proposed sparse optimization and the "pole/zero" methods.

Fig. 6 shows that the proposed method leads to less uncertainty in the implementation procedure than the "pole/zero" method.

Circuit implementation of fractional-order Jerk chaotic system

We consider the fractional-order Jerk system [59], described as

$$
\begin{cases}
\frac{d^q x}{dt^q} = y, \\
\frac{d^q y}{dt^q} = z, \\
\frac{d^q z}{dt^q} = -x - y - \beta z + F(x),
\end{cases} \tag{30}
$$

where the nonlinear function $F(x) = A\sum_{n=1}^{N_J}\mathrm{sgn}[x - (2n - 1)A] + A\sum_{m=1}^{M_J}\mathrm{sgn}[x - (2m - 1)A], N_J = M_J = 4, A = 1$ and $\mathrm{sgn}(\cdot)$ is the signum function.

When $\beta = 0.3$, a necessary condition for the fractional system to remain chaotic is keeping $q > \frac{2}{\pi}\arctan\left(\frac{\gamma}{\eta}\right) = 0.876$, where $\eta = \mathrm{Re}(\lambda_{2,3}), \gamma = \mathrm{Im}(\lambda_{2,3})$. We choose $q = 0.87$ (non-chaotic behavior) and $q = 0.88$ (chaotic behavior) to demonstrate the effectiveness of the proposed method.

The main circuit implementation of the Jerk system is depicted in Fig. 7 using OPAs and RC chain type fractances. In order to generate the $\mathrm{sgn}(\cdot)$ function in $F(x)$, the OPAs in the circuit are required to have high slew rates. Here, choosing TL081/TL084 (slew rate is 16 V/μs, output voltage swing is ±13.5 V when load resistance $R_L = 10$ kΩ and supply voltage is ±15 V), and $R0 = 1$ kΩ, thus $R6 = R0/\beta \approx 3.3$ k$\Omega, R5 = R0 = 1$ k$\Omega, R8 = 13.5$ kΩ, and $R7 = R_L = 10$ kΩ.

In the approximation of $1/s^q$, we set the maximum discrepancy $\delta = 2$ dB and bandwidth of system $\omega \in \left[10^0, 10^5\right)$ rad/s. In order to

maintain the consistency of stability between the original system and the approximation system, we introduce a scale factor G into the implementation, then the chaotic system can be rewritten as

$$
\begin{cases}
G \cdot \frac{d^q x}{dt^q} = y, \\
G \cdot \frac{d^q y}{dt^q} = z, \\
G \cdot \frac{d^q z}{dt^q} = -x - y - \beta z + F(x).
\end{cases} \tag{31}
$$

where $\tau_{\omega_r} = C_r \cdot R0 = |\widehat{H}(j\omega_r)| \cdot G$ can be regarded as the integration time constant at frequency point ω_r. Obviously, the stability condition of system (31) have not changed because all the eigenvalues are consistent with system (30) at the corresponding equilibrium point $(x_i, 0, 0)$.

Approximation using the "pole/zero" method

The integer-order approximation of $\frac{1}{s^{0.87}}$ and $\frac{1}{s^{0.88}}$ with frequency range $\omega \in \left[10^0, 10^5\right)$ rad/s, $\delta = 2$ dB are given as follows:

$$
\frac{1}{s^{0.87}} \approx \frac{6.3767(s+45.0199)(s + 2640.8921)(s + 154916.3511)}{(s+1.3030)(s+76.4344)(s+4483.6915)(s+263016.0896)}, \tag{32a}
$$

$$
\frac{1}{s^{0.88}} \approx \frac{6.2439(s+60.298)(s+4723.2662)(s+369983.0414)}{(s+1.2991)(s+101.7597)(s+7971.043)(s+624387.9966)}. \tag{32b}
$$

Therefore, the inter-order dynamical equations of them at equilibrium points can be derived by.

$$
\begin{cases}
\frac{d^4 x}{dt^4} = -\left(a_1\frac{d^3 x}{dt^3} + a_2\frac{d^2 x}{dt^2} + a_3\frac{dx}{dt} + a_4 x\right) + GK\left(\frac{d^3 y}{dt^3} + b_1\frac{d^2 y}{dt^2} + b_2\frac{dy}{dt} + b_3 y\right), \\[4pt]
\frac{d^4 y}{dt^4} = -\left(a_1\frac{d^3 y}{dt^3} + a_2\frac{d^2 y}{dt^2} + a_3\frac{dy}{dt} + a_4 y\right) + GK\left(\frac{d^3 z}{dt^3} + b_1\frac{d^2 z}{dt^2} + b_2\frac{dz}{dt} + b_3 z\right), \\[4pt]
\frac{d^4 z}{dt^4} = -GK\left(\frac{d^3 x}{dt^3} + b_1\frac{d^2 x}{dt^2} + b_2\frac{dx}{dt} + b_3 x\right) - GK\left(\frac{d^3 y}{dt^3} + b_1\frac{d^2 y}{dt^2} + b_2\frac{dy}{dt} + b_3 y\right) \\[4pt]
\quad - (a_1 + GK\beta)\frac{d^3 z}{dt^3} - (a_2 + GK\beta b_1)\frac{d^2 z}{dt^2} - (a_3 + GK\beta b_2)\frac{dz}{dt} \\[4pt]
\quad - (a_4 + GK\beta b_3)z,
\end{cases} \tag{33}
$$

where $a_1 = \sum_{i=0}^{N} p_i, a_2 = \sum_{0\leqslant i<j\leqslant N} p_i p_j, a_3 = \sum_{0\leqslant i<j<k\leqslant N} p_i p_j p_k, a_4 = \prod_{i=0}^{N} p_i, b_1 = \sum_{i=0}^{N-1} z_i, b_2 = \sum_{0\leqslant i<j\leqslant N-1} z_i z_j, b_3 = \prod_{i=0}^{N-1} z_i, N = 3$

.
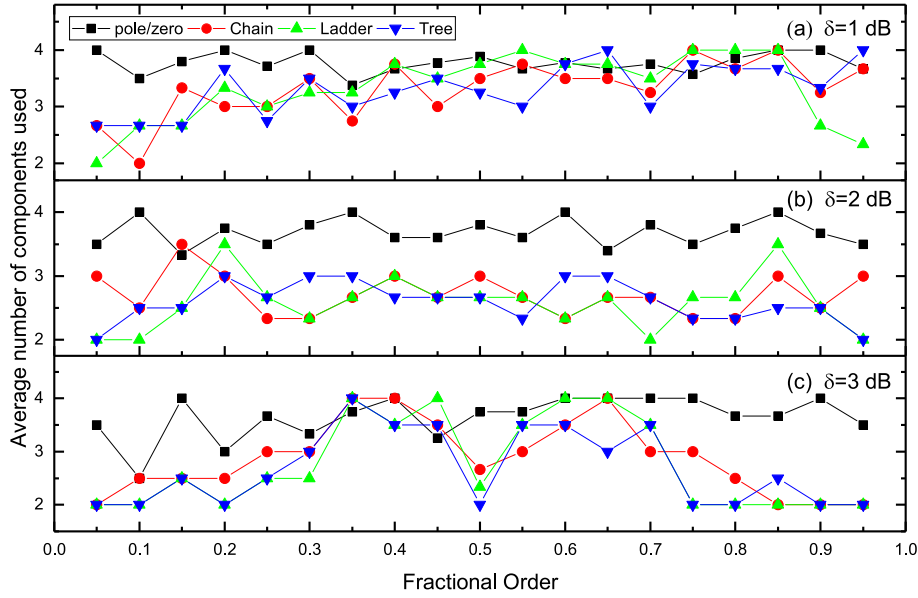
(a) The total amount of components usage.
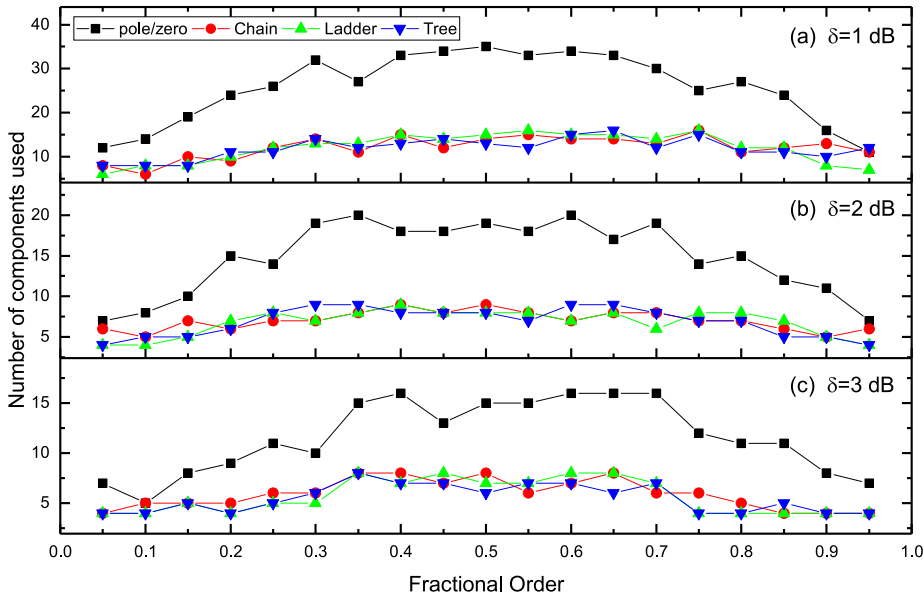
(b) The average number of components usage.

Fig. 5. The circuit complexity: comparison between the three types of fractances structure using the proposed and the "pole/zero"methods.

Then the corresponding eigenvalues of the equilibrium point $(x_i, 0, 0)$ for $q = 0.88$ and $q = 0.87$ are calculated as follows:

$$q = 0.87 \begin{cases} \lambda_1 = -76.40, \lambda_2 = -76.47, \lambda_3 = -263016.07, \lambda_4 \\ = -263016.11, \lambda_{5,6} = 0.44 \pm j2.24, \\ \lambda_{7,8} = -2.41 \pm j1.15, \lambda_{9,10} = -4483.69 \pm j0.01, \lambda_{11,12} \\ = -133789.98 \pm j229683.40 \end{cases}$$

$$q = 0.88 \begin{cases} \lambda_1 = -101.73, \lambda_2 = -101.79, \lambda_3 = -624387.97, \lambda_4 \\ = -624388.02, \lambda_{5,6} = 0.44 \pm j2.22, \\ \lambda_{7,8} = -2.40 \pm j1.15, \lambda_{9,10} = -7971.04 \pm j0.01, \lambda_{11,12} \\ = -316232.21 \pm j538928.37 \end{cases}$$

(34)

According to Tavazoei [58], a necessary condition for fractional system to remain chaotic is keeping $q > \frac{2}{\pi} \arctan\left(\frac{|\text{Im}(\lambda)|}{\text{Re}(\lambda)}\right)$. For the eigenvalues $\lambda_{9,10}, q = 0.87 < \frac{2}{\pi} \arctan\left(\frac{2.24}{0.44}\right) \approx 0.876$, and $q = 0.88 > \frac{2}{\pi} \arctan\left(\frac{2.22}{0.44}\right) \approx 0.876$, when $G = 1.97$ and 1.95, respectively, they are consistent with the stability of the original system Eqs. (32a) and (32b).

Then, choosing available E24 (5% tolerance) electronic resistors and E12 (10% tolerance) capacitors, the component values required to implement the chaotic systems of $q = 0.87$ and $q = 0.88$ are summarized in Table 3.

As shown in Fig. 8, the circuit experiments show results in agreement with the theoretical design and numerical simulations for $q = 0.88$, but are not consistent with the circuit simulation
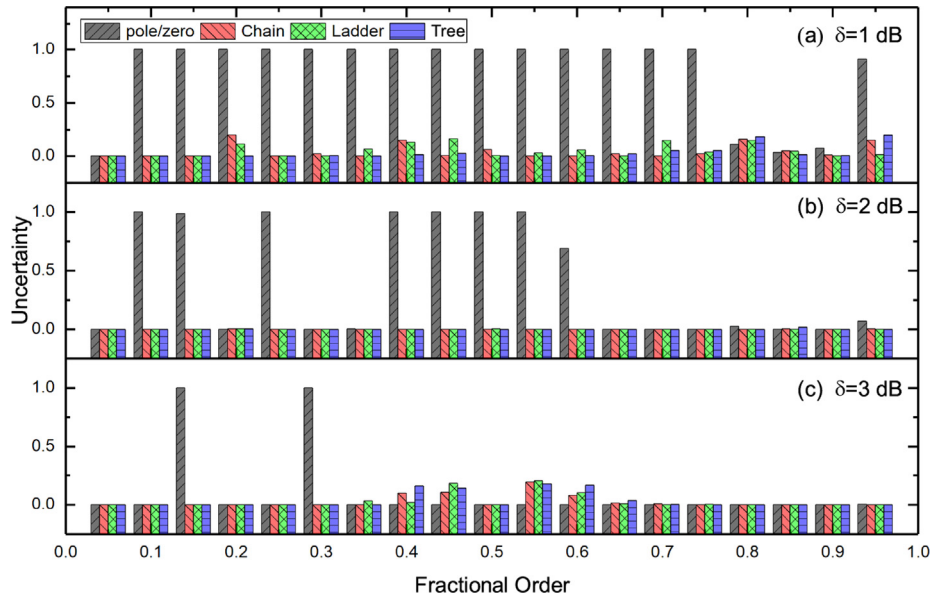
Fig. 6. The minimum system order requirement: comparison between the three types of fractances structure using the proposed and the "pole/zero" methods.
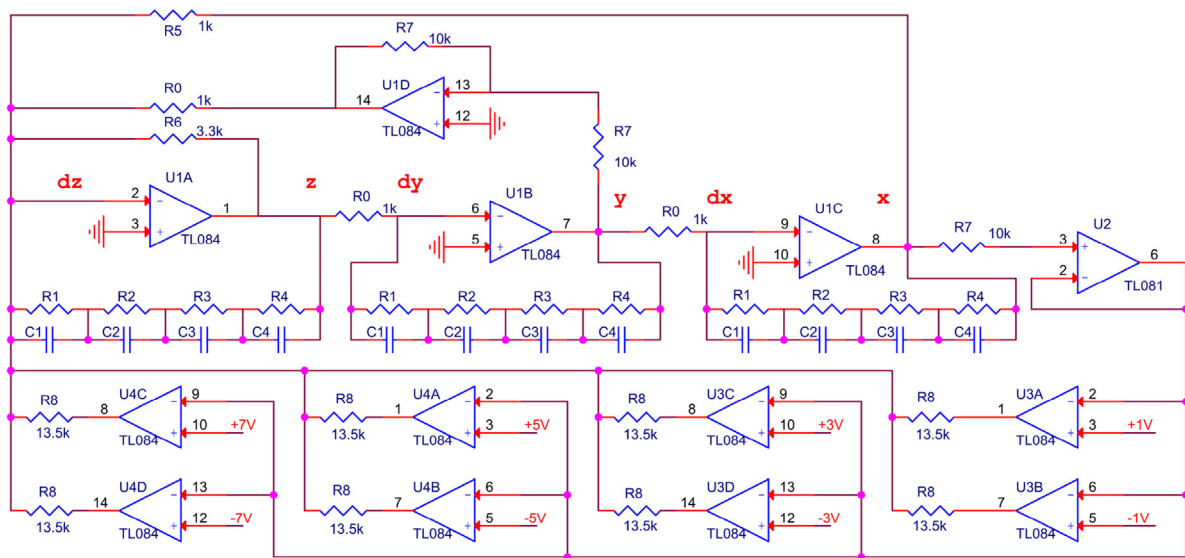

Fig. 7. Complete circuit of Jerk chaotic system with 9-scroll attractors.

Table 3
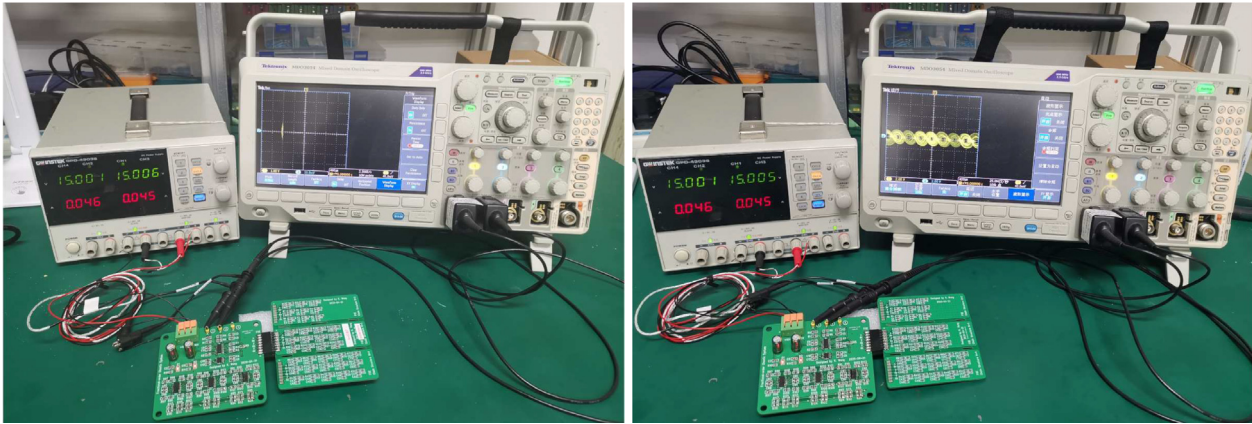The component values required to implement the chaotic systems using the "pole/zero" method.

q	ω_r (rad/s)	G	N	R1 (MΩ)	R2 (kΩ)	R3 (kΩ)	R4 (Ω)	C1 (nF)	C2 (nF)	C3 (nF)	C4 (nF)	Result
0.87	2.63×10^5	1.97	3	49.64	600.79	17.22	504.48	15.46	21.78	12.95	7.54	Fake chaotic behavior (simulation)
				47 + 2.4	560 + 39	16 + 1.2	470 + 33	15	18 // 3.3	12// 0.82	6.8 // 0.68	Non-chaotic behavior (hardware)
0.88	5×10^4	1.95	3	13.42	119.35	2.55	55.48	57.35	82.34	49.15	28.87	Chaotic behavior
				10 + 3.3	110 + 9.1	2.4 + 0.15	51	56	82	47 // 1.8	27 // 1.8	

for $q = 0.87$. The inconsistency between the simulation results and the theoretical design is most likely caused by amplitude and phase errors and can be improved by increasing the order of the approximation system. However, the actual circuit is consistent with the theoretical design, which may be caused by the limited bandwidth of the circuit. Choose the circuit output 'x' as the horizontal axis input and the circuit output 'z' as the vertical axis input, then the observation of simulations by using NI Multisim software

and experiments by using oscilloscope (Tektronix MDO3054 500 MHz) are shown in Figs. 9 (a, b) and Figs. 8 (c,d), respectively.
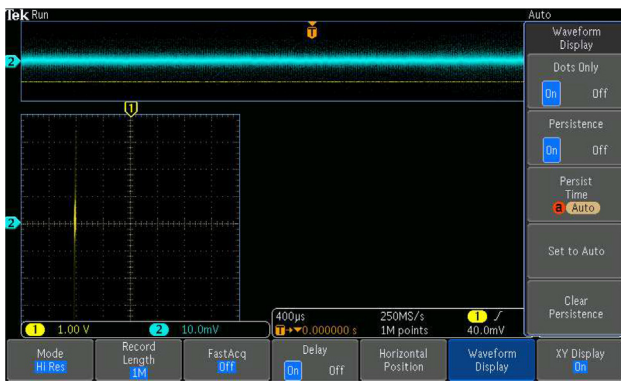
Approximation using the proposed method

Now we choose the same fractional order and frequency range as the "pole/zero" method and we substitute the uncertainty criteria by Definition 3. The component values required to implement
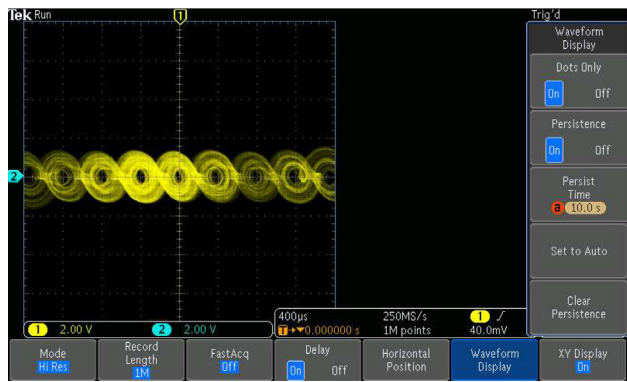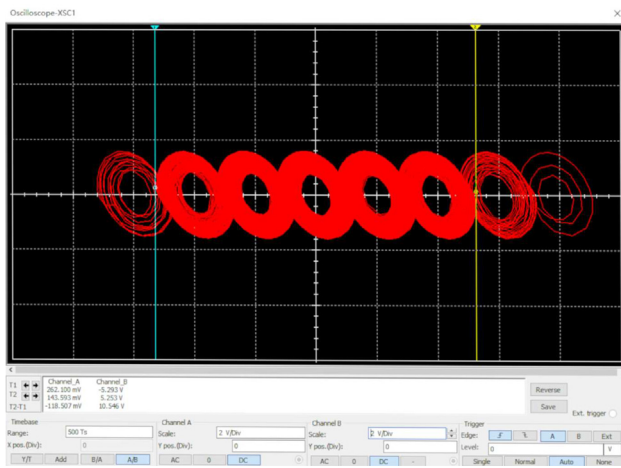
(a) $q = 0.87$
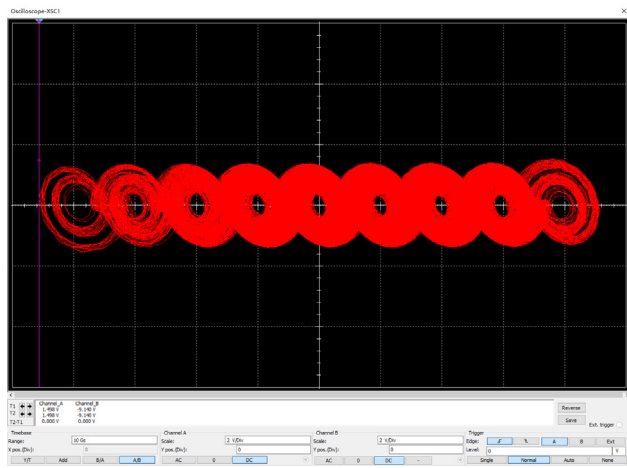
(b) $q = 0.88$

(c) $q = 0.87$

(d) $q = 0.88$

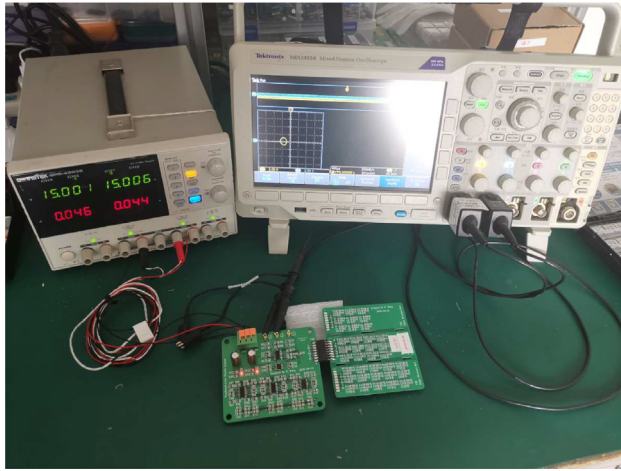**Fig. 8.** Hardware circuit implementation using the "pole/zero" method.
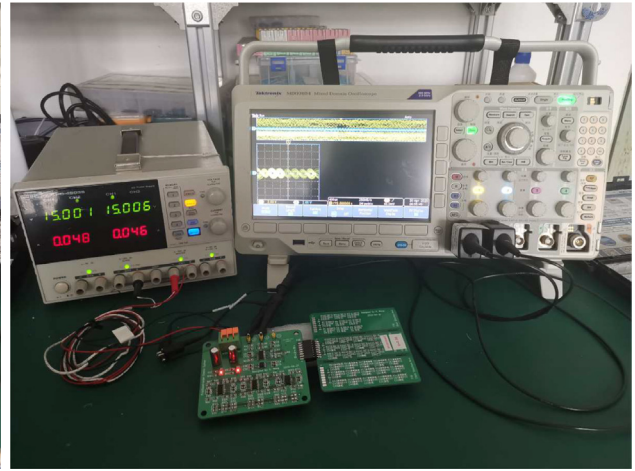

(a) $q = 0.87$

(b) $q = 0.88$

Fig. 9. Simulation observations of Jerk chaotic system with $q = 0.87$ and 0.88.

Table 4
The component values required to implement the chaotic systems using the proposed method.
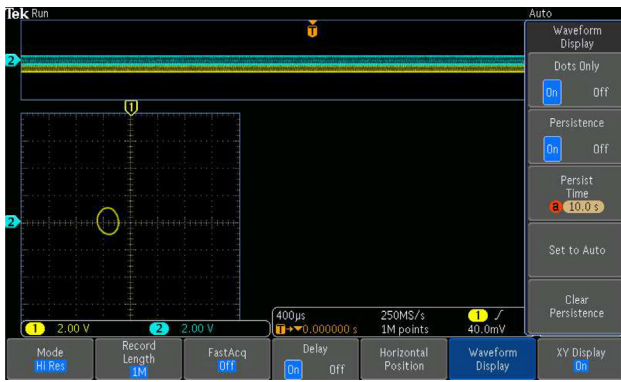
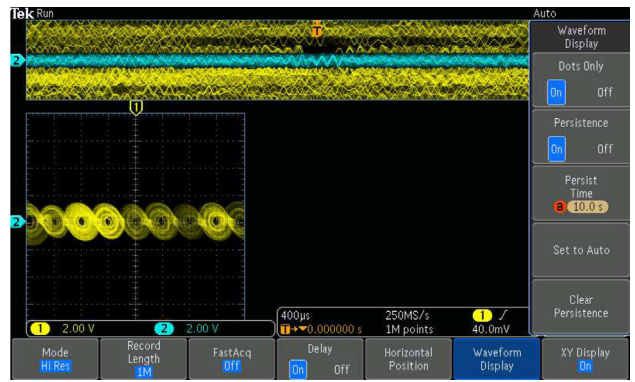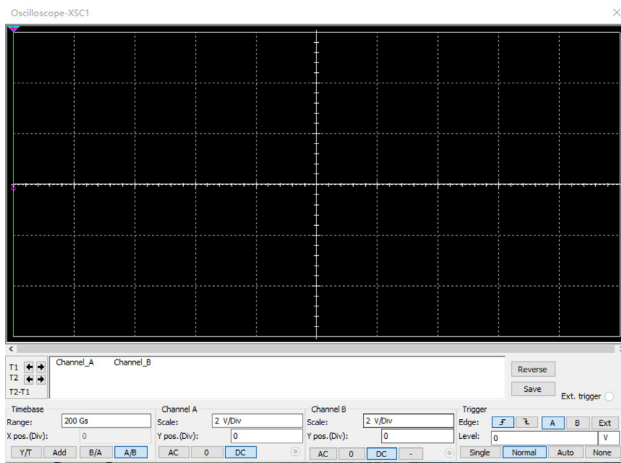| q	C_r	N	$R1$ (MΩ)	$R2$ (kΩ)	$R3$ (kΩ)	$R4$ (Ω)	$C1$ (nF)	$C2$ (nF)	$C3$ (nF)	$C4$ (nF)	Result
0.87	1.88×10^{-8}	3	100	1200	34.5	1000	7.67	10	6.8	3.9	Non-chaotic behavior
			100	1200	33 + 1.5	1000	6.8// 0.82	10	6.8	3.9	
0.88	1.797×10^{-7}	3	20	180	3.82	83	39	53.8	33	19.2	Chaotic behavior
			20	180	3.6 + 0.22	82	39	47// 6.8	33	18 //1.2	

(a) $q = 0.87$ (b) $q = 0.88$
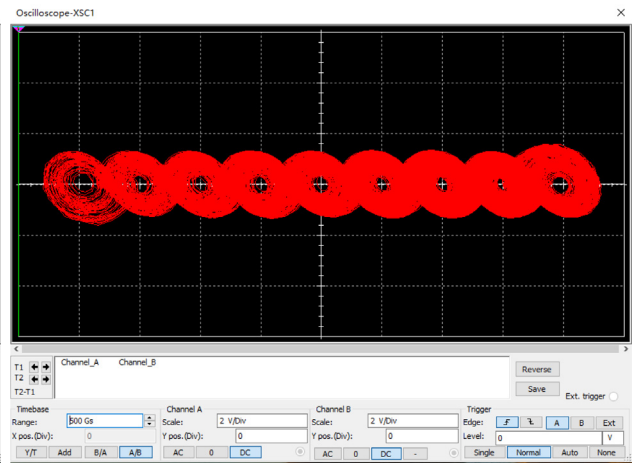
(c) $q = 0.87$ (d) $q = 0.88$

Fig. 10. Hardware circuit implementation using the proposed method.

(a) $q = 0.87$ (b) $q = 0.88$

Fig. 11. Simulation observations of Jerk chaotic system with $q = 0.87$ and 0.88.

the chaotic systems of $q = 0.87$ and $q = 0.88$ with $\delta = 2$ dB are summarized in Table 4.

As shown in Figs. 10 and 11, the circuit experiments show results in agreement with the theoretical designs and numerical simulations both for $q = 0.87$ and 0.88. The proposed method can achieve the same approximation accuracy with fewer compo-nents. Since the necessary condition (Definition 3) of chaotic sys-tem are considered in the optimization process, the problem of inconsistency with the theoretical design can be avoided. In gen-eral, once the estimated value of implementation uncertainty is calculated, the uncertainty in the realization process can be reduced to improve the circuit behavior by the following strategy:

(1) Select standard components with relative higher precision level, such as E96, E192;
(2) Adjust the scaling factor C_r to meet the condition of chaos in fractional order system;
(3) Adjust the value of R0 to affect the integration time constant.

Conclusion and discussion

This paper described a novel parameter selection method based on sparse optimization for chaotic circuit system implementation. Furthermore, an uncertainty measurement method of the implementation procedure was formulated. To the authors best knowledge, this is the first work that considers the uncertainty in the circuit implementation when using standard electronic components. Indeed, the method gives a feasible circuit parameter optimization method. The new approach is very helpful for implementing arbitrary fractional chaotic systems with commercially available components while the system accuracy and complexity can be analyzed assertively.

The experiments comparing three types of fractances structure demonstrated that the proposed selection method for the parameters can find a low-order circuit system and a minimum number for the combination of standard components when representing a given fractional order fractance.

This paper focused on the implementation of fractional order fractance circuits. Nonetheless, it can be easily used and integrated into specific chaotic circuit design and has great potential to discover more structures of high-complexity chaotic circuits using optimization algorithms. It is also possible to introduce other criteria in the objective function Eq. (17) for system level optimization, such as, for example, the criteria of quantitative determination of chaotic behavior, synchronization and stabilization.

Declaration of Competing Interest

The authors declare that they have no known competing financial interests or personal relationships that could have appeared to influence the work reported in this paper.

Compliance with Ethics Requirements

This article does not contain any studies with human or animal subjects.

Author Contributions

In this paper, Juan Yao and Kunpeng Wang designed and programmed the proposed algorithm, and write this paper; Pengfei Huang participated the algorithm designation and test the proposed method. Liping Chen participated the algorithm design, algorithm programming and paper writing processes; J. A. Tenreiro Machado provided technical support and revised the paper. All authors have read and approved the final manuscript.

Acknowledgment

References

[1] Petráš I. Fractional-order nonlinear systems: modeling, analysis and simulation. Springer; 2011.
[2] Podlubny I. Fractional-order system and $PI^\lambda D^\mu$-controllers. IEEE Trans Autom Control 1999;44(1):208–14.
[3] Oustaloup A, Moreau X, Nouillant M. The CRONE suspension. Control Eng Pract 1996;4(8):1101–8.
[4] Oustaloup A. Diversity and non-integer differentiation for system dynamics. Wiley; 2014.
[5] Machado JT, Lopes AM. Fractional-order modeling of a diode. Commun Nonlinear Sci Numer Simul 2019;70:343–53.
[6] Elwakil AS. Fractional-order circuits and systems: an emerging interdisciplinary research area. IEEE Circ Syst Mag 2010;10(4):40–50.
[7] Almeida LB. The fractional Fourier transform and time-frequency representations. IEEE Trans Signal Process 1994;42(11):3084–91.
[8] Akhmet M, Fen MO. Replication of chaos in neural networks, economics and physics. Springer; 2016.
[9] Kiani-B A, Fallahi K, Pariz N, Leung H. A chaotic secure communication scheme using fractional chaotic systems based on an extended fractional Kalman filter. Commun Nonlinear Sci Numer Simul 2009;14(3):863–79.
[10] Muthukumar P, Balasubramaniam P. Feedback synchronization of the fractional order reverse butterfly-shaped chaotic system and its application to digital cryptography. Nonlinear Dyn 2013;74:1169–81.
[11] Chua LO, Komuro M, Matsumoto T. The double scroll family. IEEE Trans Circ Syst 1986;33(11):1072–118.
[12] Pham VT, Kingni ST, Volos C, Jafari S, Kapitaniak T. A simple three-dimensional fractional-order chaotic system without equilibrium: Dynamics, circuitry implementation, chaos control and synchronization. Int J Electron Commun (AEÜ) 2017;78:220–7.
[13] Zhou P, Huang K. A new 4-d non-equilibrium fractional-order chaotic system and its circuit implementation. Commun Nonlinear Sci Numer Simulat 2014;19:2005–11.
[14] Akgul A. Chaotic oscillator based on fractional order memcapacitor. J Circ, Syst Comput 2019;28:1950239.
[15] Akgul A, Arslan C, Aricioglu B. Design of an interface for random number generators based on integer and fractional order chaotic systems. Chaos Theory Appl 2019;1:9:1–18.
[16] Bourouba B, Ladaci S, Chaabi A. Reduced-order model approximation of fractional-order systems using differential evolution algorithm. J Control, Autom Electr Syst 2018;29:32–43.
[17] Khanra M, Pal J, Biswas K. Rational approximation and analog realization of fractional order transfer function with multiple fractional powered terms. Asian J Control 2013;15:723–35.
[18] Baranowski J, Pauluk M, Tutaj A. Analog realization of fractional filters: Laguerre approximation approach. Int J Electron Commun (AEÜ) 2017;81:1–11.
[19] Machado JT, Lopes AM. Multidimensional scaling locus of memristor and fractional order elements. J Adv Res 2020;25:147–157.
[20] Samavati H, Hajimiri A, Shahani AR, Nasserbakht GN, Lee TH. Fractal capacitors. IEEE J Solid-State Circ 1998;33(12):2035–41.
[21] Jesus IS, Machado JT. Development of fractional order capacitors based on electrolyte processes. Nonlinear Dyn 2009;56:45–55.
[22] Caponetto R, Dongola G, Fortuna L, Petráš I. Fractional order systems: modeling and control applications. World Scientific; 2010.
[23] Schäfer I, Krüger K. Modelling of lossy coils using fractional derivatives. J Phys D: Appl Phys 2008;41(4):045001.
[24] Kawaba K, Nazri W, Aun HK, Iwahashi M, Kambayashi N. A realization of fractional power-law circuit using OTAs. In: IEEE Asia-Pacific conference on circuits and systems. Microelectronics and integrating systems., IEEE, Chiangmai, Thailand; 1998. p. 249–52.
[25] Ramachandran V, Gargour CS, Ahmadi M. Cascade realisation of the irrational immittance $s^{1/2}$. IEE Proc G-Electron Circ Syst 1985;132(2):64–7.
[26] Carlson GE, Halijak CA. Approximation of fractional capacitors $(1/s)^{(1/n)}$ by a regular Newton process. IEEE Trans Circ Theory 1964;11(2):210–3.
[27] Wang JC. Realizations of generalized Warburg impedance with RC ladder networks and transmission lines. J Electrochem Soc 1987;134(8):1915–20.
[28] Charef A. Modeling and analog realization of the fundamental linear fractional order differential equation. Nonlinear Dyn 2006;46:195–210.
[29] Roy SCD. On the realization of a constant-argument immittance or fractional operator. IEEE Trans Circ Theory 1967;14(3):264–74.
[30] Oldham KB, Zoski CG. Analogue instrumentation for processing polarographic data. J Electroanal Chem Interfacial Electrochem 1983;157(1):27–51.
[31] Fouda ME, Soltan A, Radwan AG, Soliman AM. Fractional-order multi-phase oscillators design and analysis suitable for higher-order PSK applications. Analog Integr Circ Sig Process 2016;87(2):301–12.
[32] AbdelAty AM, Elwakil AS, Radwan AG, Psychalinos C, Maundy BJ. Approximation of the fractional-order laplacian s^α as a weighted sum of first-order high-pass filters. IEEE Trans Circ Syst II Exp Briefs 2018;65:1114–8.
[33] Barbosa RS, Machado JT, Ferreira IM. Pole-zero approximations of digital fractional-order integrators and differentiators using signal modeling techniques. IFAC Proc Vol 2005;38(1):309–14.
[34] Scherer R, Kalla SL, Tang Y, Huang J. The Grünwald-Letnikov method for fractional differential equations. Comput Math Appl 2011;62(3):902–17.

[35] Al-Alaoui MA. Novel digital integrator and differentiator. Electron Lett 1993;29 (4):376–8.

[36] ShahaRoh DK, Chaurasiya RB, Vyawahare VA, Pichhode K, Patil MD. FPGA implementation of fractional-order chaotic systems. Int J Electron Commun (AEÜ) 2017;78:245–57.

[37] Pano-Azucena AD, Tlelo-Cuautle E, Rodriguez-Gomez G, de la Fraga LG. FPGA-based implementation of chaotic oscillators by applying the numerical method based on trigonometric polynomials. AIP Adv 2018;8:075217.

[38] Vinagre BM, Podlubny I, Hernández A, Feliu V. Some approximations of fractional order operators used in control theory and applications. Fract Calc Appl Anal 2000;3(3):231–48.

[39] Kartci A, Herencsar N, Machado JT, Brancik L. History and progress of fractional-order element passive emulators: a review. Radioengineering.

[40] Matsuda K, Fujii H. H^{∞} optimized wave-absorbing control: analytical and experimental results. J Guid, Control, Dynam 1993;16(6):1146–53.

[41] Oustaloup A, Levron F, Mathieu B, Nanot FM. Frequency-band complex noninteger differentiator: characterization and synthesis. IEEE Trans Circ Syst I: Fundam Theory Appl 2000;47(1):25–39.

[42] Charef A, Sun HH, Tsao YY, Onaral B. Fractal system as represented by singularity function. IEEE Trans Autom Control 1992;37(9):1465–70.

[43] Sheng H, Chen Y, Qiu T. Fractional processes and fractional-order signal processing: techniques and applications. Springer; 2012.

[44] Pearn W, Hung H, Peng N, Huang C. Testing process precision for truncated normal distributions. Microelectron Reliab 2007;47(12):2275–81.

[45] IEC 60063: 2015 preferred number series for resistors and capacitors, Standard, International Electrotechnical Commission (IEC); 2015.

[46] Johnson NL, Kotz S, Balakrishnan N. Continuous Univariate Distributions. 2nd ed. Wiley; 1995.

[47] Jeroslow RC. There cannot be any algorithm for integer programming with quadratic constraints. Oper Res 1973;21(1):221–4.

[48] Conn AR, Gould N, Toint PL. A globally convergent Lagrangian barrier algorithm for optimization with general inequality constraints and simple bounds. Math Comput 1997;66(217):261–88.

[49] Goldberg DE, Holland JH. Genetic algorithms and machine learning. Mach Learn 1988;3:95–9.

[50] Machado JT. Optimal tuning of fractional controllers using genetic algorithms. Nonlinear Dyn 2010;62:447–52.

[51] Machado JT, Galhano AM, Oliveira AM, Tar JK. Optimal approximation of fractional derivatives through discrete-time fractions using genetic algorithms. Commun Nonlinear Sci Numer Simul 2010;15:482–90.

[52] Machado JT, Galhano AM. Fractional order inductive phenomena based on the skin effect. Nonlinear Dyn 2012;68:107–15.

[53] Rohatgi VK, Saleh AME. An introduction to probability and statistics. Wiley; 2015.

[54] Hinkley DV. On the ratio of two correlated normal random variables. Biometrika 1969;56(3):635–9.

[55] Kroese DP, Taimre T, Botev ZI. Handbook of Monte Carlo Methods. Wiley; 2011.

[56] Botev ZI, L'Ecuyer P. Simulation from the normal distribution truncated to an interval in the tail. In: 10th EAI International Conference on Performance Evaluation Methodologies and Tools, Taormina Italy; 2016.

[57] Chopin N. Fast simulation of truncated Gaussian distributions. Stat Comput 2011;21:275–88.

[58] Tavazoei MS, Haeri M. A necessary condition for double scroll attractor existence in fractional-order systems. Phys Lett A 2007;367:102–13.

[59] Chen L, Pan W, Wu R, Wang K, He Y. Generation and circuit implementation of fractional-order multi-scroll attractors. Chaos, Solit Fract 2016;85:22–31.